Robotica (2015) volume 33, pp. 1718–1730. © Cambridge University Press 2014
doi:10.1017/S0263574714001015

Image-based robotic control with unknown camera parameters and joint velocities

Changchun Hua, Yinjuan Liu and Yana Yang

Department of Automation, Institute of Electrical Engineering, Yanshan University, Qinhuangdao City 066004, China

(Accepted March 26, 2014. First published online: April 29, 2014)

SUMMARY

A new image-based controller is proposed for the robotic system with the joint velocity signals unavailable. The Immersion and Invariance (I&I) observer is applied to estimate the unknown velocity information. Compared with the general velocity observer, the I&I observer can estimate the unknown velocity exponentially. We consider the case that the exact camera parameters are not known. The corresponding adaptive controller is designed for the robot system and the stability is rigorously proven by using Lyapunov theorem. Finally, simulations are performed and the results show the effectiveness of the proposed control approach.

KEYWORDS: Image-based; Robot control; I&I velocity observer; Unknown camera parameters.

1. Introduction

Visual servoing has attracted more and more researchers' attention during the past decades. Many servoing schemes have been proposed, see ref. [1 and the references therein] . Based on the hand–eye relation, visual servo systems have two types of camera configurations: eye-in hand (moving camera)[2–6] and eye-to-hand (fixed camera).[7,8] Visual servoing can also be classified into two broad classes: position-based visual servoing and image-based visual servoing. Position-based schemes define the error system between the current position and the desired one in the robot workspace, while image-based schemes define the error system based on the camera screen coordinate. When we consider the tasks the robot performed, we can classify them into visual tracking and visual positioning. Visual tracking is that the visual positioning regulates the end-effector to an objective position based on visual information. The robot end-effector tracks a desired moving object via visual tracking.

Many nonlinear control schemes have been proposed for the visual tracking control of the robot system. Astolfi and Ortega[9] proposed a new adaptive visual servoing scheme based on the notion of system immersion and manifold invariance (I&I). Akella[10] proposed an adaptive control scheme in the presence of parametric uncertainties . Liu *et al.*[11,12] proposed a new visual servoing scheme based on the notion of depth-independent interaction matrix. In ref. [13], a new controller was presented to regulate a set of feature points on the image plane to the desired positions by controlling the motion of a robot manipulator in uncalibrated environment. Moreover, this controller can also cope with the unknown camera robot parameters. Although there are so many regulation schemes in this field, almost all of these need the assumption that the velocities of robot joints are known in advance. Su *et al.*[14] proposed a regulation method under the consideration that the robot velocities are unavailable. The so-called dirty " derivative" technique was applied to estimate robot velocities, and asymptotical convergence results were given. Liang *et al.*[15] proposed a sliding mode observer to estimate joint velocities. An adaptive visual servoing scheme with uncalibrated camera was proposed in ref. [16] for the case that robot parameters are unknown and the velocity signal is not available. In ref. [17], a reduced-order nonlinear observer was developed to estimate the distance from a moving camera to a feature point on a static object.

* Corresponding author. E-mail:cch@ysu.edu.cn

Astolfi and Ortega[9] in 2003 were the first to propose the notion of system immersion and (manifold) invariance; they also designed a velocity observer based on this notion for mechanical system. Unlike other velocity observer, this observer was globally convergent. In ref. [18], we showed that the robot can successfully accomplish the positioning task with I&I joint velocity observer. But similar to many previous works, we supposed that all the parameters of the robot and the camera are exactly known in advance. In this work, we will develop our previous work to the case that all camera parameters are unknown and the depth-independent interaction is used to linearize camera parameters with the use of a Jacobian matrix. The main contributions of this work are as follows: (i) an I&I velocity observer is constructed to estimate the velocities, and the estimation error is shown to be exponentially convergent; (ii) an adaptive observer control design method is proposed based on the estimated velocities and (iii) by using the Lyapunov stability theory, the stability of the closed-loop system is proved in the rigorous sense.

This paper is organized as follows. Section 2 presents preliminary knowledge for the visual servoing model with the related properties. Section 3 introduces an I&I velocity observer. In Section 4, we design a controller with the joint velocities estimated by an I&I observer, and analyse the stability of the whole closed-loop system. Simulation results are given in Section 5 to illustrate the performance of the proposed scheme. Section 6 concludes with a summary of the obtained results.

Notation: Throughout this paper, the norm of vector is denoted by $|\cdot|$ and the norm of matrix is denoted by $\|\cdot\|$, $\lambda_{\min}(K)$ and $\lambda_{\max}(K)$ denote the minimal and maximal eigenvalues of matrix K respectively.

2. Problem Formulation

The problem considered in this study is to design a new controller to regulate the end-effector of the manipulator to a target position. Here the camera is fixed at a certain place where it can always capture manipulator's image. Moreover, joints' velocities and camera parameters are supposed to be unknown. In this paper, we suppose that the end-effector of the manipulator is always in camera's field of view. Then some knowledge of robot system and camera model is presented.

2.1. Robot system

The robot system considered in this paper is an n-link eye-to-hand manipulator. Generally, an n-degree of freedom robot manipulator system governed by the following dynamics in the absence of friction and other disturbance is as follows:

$$M(q)\ddot{q} + C(q,\dot{q})\dot{q} + G(q) = \tau, \tag{1}$$

where $q(t)$, $\dot{q}(t)$, $\ddot{q}(t) \in R^n$ denote the vectors of joint displacements, velocities and accelerations respectively, $M(q) \in R^{n\times n}$ represents the symmetric positive definite manipulator inertial matrix, $C(q,\dot{q}) \in R^{n\times n}$ is the centripetal and Coriolis torque matrix, $G(q) \in R^n$ represents the gravitational torque vector and $\tau \in R^n$ is the input torque vector.

The robot dynamics has the following well-known structural properties:

Property 1. For a manipulator with revolute joints, the inertia matrix $M(q)$ is symmetric positive-definite and has the following upper and lower bounds:

$$0 < \lambda_{\min}(M(q))I \le M(q) \le \lambda_{\max}(M(q))I \le \infty, \tag{2}$$

where $I \in R^{n\times n}$ is the identity matrix.

Property 2. The matrix $\dot{M}(q) - 2C(q,\dot{q})$ is skew-symmetric and satisfies

$$q^T[\dot{M}(q) - 2C(q,\dot{q})]q = 0, \forall q \in R^n. \tag{3}$$

In this paper, a factorization of inertia matrix borrowing from Liang *et al.*[15] is introduced,

$$M(q) = T^T(q)\,T(q), \tag{4}$$

https://doi.org/10.1017/S0263574714001015 Published online by Cambridge University Press

where $T(q) \in R^{n\times n}$ always exists and is a full rank matrix because that $M(q)$ is a symmetric positive definite matrix. Besides, define the mappings $L : R \to R^{n\times n}$ and $F : R^n \times R^n \to R^n$ as

$$L(q) = T^{-1}(q), F(q, \tau) = L^T(q)(\tau - G(q)) \tag{5}$$

with $y = q$, $x = T(q)\dot{q}$, the robot system (1) can be transformed into the following form:

$$\begin{aligned} \dot{y} &= L(y)x, \\ \dot{x} &= S(y, x)x + F(y, \tau), \end{aligned} \tag{6}$$

the mapping $S : R^n \times R^n \to R^{n\times n}$ is defined as

$$S = (\dot{T} - T^{-T}C)T^{-1}, \tag{7}$$

where S satisfies the following three properties:

(i) S is skew-symmetric, i.e., $S + S^T = 0$.

(ii) S is linear in the second argument, i.e., $S(y, \alpha_1 x + \alpha_2 \bar{x}) = \alpha_1 S(y, x) + \alpha_2 S(y, \bar{x})$ for all $y, x, \bar{x} \in R^n$ and $\alpha_1, \alpha_2 \in R$.

(iii) There exists a mapping $\bar{S} : R^n \times R^n \to R^{n\times n}$ satisfying $S(x, x)y = \bar{S}(x, y)x$.

See ref. [19] for the proof of the properties.

As we all know, the robot dynamics describes the relationship between joint displacements and input torques, and the robot differential kinematics describes the relationship between the velocities of joints and the velocities of robot end-effector as follows,

$$\dot{X} = J_A(q)\dot{q}, \tag{8}$$

where X, $\dot{X} \in R^3$ represent the robot end-effector position and velocity vectors respectively. $J_A(q)$ is an analytical robot Jacobian matrix.

2.2. Camera system

In this paper, we use the depth-independent interaction matrix to denote imaging model. Three coordinates are set up to denote the system: robot base coordinate, end-effector coordinate and camera coordinate. We consider that the object can be characterized by a set of feature points. The position of the feature point in the camera screen is $\varsigma = [u, v]$. C_z is the depth of the feature points with respect to the camera coordinate. The relationship between these is given as follows:

$$\begin{pmatrix} \varsigma \\ 1 \end{pmatrix} = \frac{1}{C_z} N \begin{pmatrix} X \\ 1 \end{pmatrix}, \tag{9}$$

where N is a 3×4 matrix, which is called a perspective matrix, and N contains all the parameters of the camera. From Eq. (9), we get

$$\varsigma = \frac{1}{C_z} PX, \tag{10}$$

where matrix P is a sub-matrix of N and

$$P = \begin{pmatrix} N_{11} & N_{12} & N_{13} \\ N_{21} & N_{22} & N_{23} \end{pmatrix}, \tag{11}$$

then we have

$$\dot{\varsigma} = \frac{1}{C_z}(P\dot{X} - \varsigma\dot{C}_z) = \frac{1}{C_z} A(t)\dot{q}(t), \tag{12}$$

https://doi.org/10.1017/S0263574714001015 Published online by Cambridge University Press

where $\frac{1}{C_z} A(t)$ is called the depth-independent matrix and

$$A(t) = \left(P - \varsigma(t) N_3^T\right) J_A(q(t)) \tag{13}$$

from Liu *et al.*,[11] the depth-independent matrix can be linearized to the camera parameters and has the following properties:

Property 3. Depth-independent matrix $A(t)$ has a rank of 2 if the perspective matrix N is 3.

Property 4. For any 2×1 vector ρ, there is $A(t)\rho = Y(\rho, \varsigma(t))\theta$, where $Y(\rho, \varsigma(t))$ is a matrix independent of the camera intrinsic or extrinsic parameters, and θ is an unknown vector.

Our objective in this paper is to design a controller for the robot system (1) guaranteeing that as $t \to \infty$, $\tilde{\varsigma} = \varsigma - \varsigma_d \to 0$, $\hat{q} \to 0$ (this implies $\dot{q} \to 0$ under the assumption that the observer can estimate the virtual velocities successfully), ς, ς_d, $\tilde{\varsigma}$ stand for the current image position, desired image position and image position error respectively.

3. Immersion and Invariance Velocity Observer

In this section, the I&I observer will be designed to estimate x which has been defined in (6).

We propose the following manifold for system (7),

$$s = \xi - x + \beta(y, \hat{y}, \hat{x}), \tag{14}$$

where ξ, $\hat{y}$, $\hat{x} \in R^n$ are the variables of the observer, the mapping $\beta : R^{3n} \to R^n$ is a nonlinear function vector to be defined. If we can prove that the manifold s is attractive and invariant, then x can be estimated by $\xi + \beta$. We differentiate s and have

$$\dot{s} = \dot{\xi} - \dot{x} + \dot{\beta} = \dot{\xi} - S(y, x)x - F + \nabla_y \beta \hat{y} + \nabla_{\hat{y}} \beta \hat{y} + \nabla_{\hat{x}} \beta \hat{x}. \tag{15}$$

Let

$$\dot{\xi} = F - \nabla_{\hat{y}} \beta \hat{y} - \nabla_{\hat{x}} \beta \hat{x} + S(y, \xi + \beta)(\xi + \beta) - \nabla_y \beta L(y)(\xi + \beta) \tag{16}$$

and

$$\nabla_y \beta = [k_1 I + \bar{S}(y, \xi + \beta)] L^{-1}(y), \; k_1 > 0, \tag{17}$$

where s is attractive and invariant. However, solving (17) is a daunting task and β may not exist. In ref. [19], the authors proposed an approximation solution of $\nabla_y \beta$.

Give the solution of $\nabla_y \beta$ as

$$\beta(y, \hat{y}, \hat{x}) = \int_0^{y_1} H_1([s, \hat{y}_2, \ldots, \hat{y}_n], \hat{x})\, ds + \cdots + \int_0^{y_n} H_n([\hat{y}_1, \ldots, \hat{y}_{n=1}, s], \hat{x})\, ds, \tag{18}$$

where

$$H(y, \xi + \beta) = [H_1(y, \xi + \beta) \cdots H_n(y, \xi + \beta)], \tag{19}$$

we get

$$\dot{s} = (S - k_1) z + (\triangle_y + \triangle_x) L(y) z \tag{20}$$

https://doi.org/10.1017/S0263574714001015 Published online by Cambridge University Press

such that

$$\triangle_y (y, x, 0) = 0, \quad \triangle_x (y, \hat{x}, 0) = 0. \tag{21}$$

As S is skew-symmetric and $k_1 > 0$, $\triangle_y$ and $\triangle_x$ play the role of disturbances that will be dominated by a dynamic scaling as follows:

$$\eta = \frac{1}{r} z. \tag{22}$$

Differentiating η yields

$$\dot{\eta} = (S - k_1 I)\, \eta + (\triangle_y + \triangle_x) L (y)\, \eta - \frac{\dot{r}}{r} \eta. \tag{23}$$

Define $V_1 = \frac{1}{2} |\eta|^2$, and its time derivative is

$$\dot{V}_1 = - \left(k_1 + \frac{\dot{r}}{r} \right) |\eta|^2 - \eta^T \left(\triangle_y + \triangle_x \right) L (y)\, \eta. \tag{24}$$

Applying Young's inequality and letting

$$\dot{r} = - \frac{k_1}{4} (r - 1) + \frac{r}{k_1} (\| \triangle_y L \|^2 + \| \triangle_x L \|^2) \quad r(0) \geq 1, \tag{25}$$

one has

$$\dot{V}_1 \leq - \left(\frac{k_1}{2} - \frac{k_1}{4} \frac{r - 1}{r} \right) |\eta|^2 \leq - \frac{k_1}{4} |\eta|^2 . \tag{26}$$

Thus, η-subsystem is globally exponentially stable (GES), if $r(t) \in L_\infty$ is proved, $z = 0$ will also be GES. Before going through the proof, we firstly analyse the stability of e_y and e_x. One has

$$\begin{aligned} \dot{\hat{y}} &= L (y) (\xi + \beta) - \psi_1 (y, r)\, e_y, \\ \dot{\hat{x}} &= F + S (y, \xi + \beta) (\xi + \beta) - \psi_2 (y, r)\, e_x, \end{aligned} \tag{27}$$

where ψ_1, ψ_2 will be defined later. With (6) and (16), the error systems are

$$\begin{aligned} \dot{e}_y &= Lz - \psi_1 e_y, \\ \dot{e}_x &= \nabla_y \beta L z - \psi_2 e_x. \end{aligned} \tag{28}$$

To prove the stability of e_y and e_x, we define the following Lyapunov function:

$$V_2 = V_1 + \frac{1}{2} (|e_x|^2 + |e_y|^2). \tag{29}$$

Differentiating V_2 along (26) and (28) gives

$$\begin{aligned} \dot{V}_2 \leq & - \left(\frac{k_1}{4} - 1 \right) |\eta|^2 - \left(\psi_1 - \frac{r^2}{2} \|L\|^2 \right) |e_y|^2 \\ & - \left(\psi_2 - \frac{r^2}{2} \left\| \nabla_y \beta \right\|^2 \|L\|^2 \right) |e_x|^2 . \end{aligned} \tag{30}$$

https://doi.org/10.1017/S0263574714001015 Published online by Cambridge University Press

Selecting $k_1 = 4(1+\psi_3)$, $\psi_1 = \frac{r^2}{2}\|L\|^2 + \psi_4$ and $\psi_2 = \frac{r^2}{2}\left\|\nabla_y \beta\right\|^2 \|L\|^2 + \psi_5$, with ψ_3, ψ_4, $\psi_5 > 0$, we obtain

$$\dot{V}_2 \leq -\psi_3 |\eta|^2 - \psi_4 \left|e_y\right|^2 - \psi_5 |e_x|^2 . \tag{31}$$

Based on (29) and (31), one knows that e_x and e_y converge to zero exponentially. In the next section we will prove that $r(t) \in L_\infty$.

Remark 1. In this section, we investigate the observer design problem. It is shown that the resultant closed-loop system is GES. The parameters ψ_3, ψ_4, ψ_5 will be defined in the next section.

4. Control Design

In this section, the control scheme with robotic joint velocities estimated by the I&I observer will be presented. The adaptive control method will also be given to estimate the unknown camera parameters. Some parameters of the observer will be determined in this part. We will show that the positioning error converges to zero asymptotically with our control scheme.

Firstly, a simple PD-like controller for robot system (1) is proposed. The controller is given as follows:

$$\tau = G(q) - K_v \hat{\dot{q}} - \hat{A}^T K_p \tilde{\varsigma} \tag{32}$$

with

$$\hat{\dot{q}} = L(y)x, \tag{33}$$

$$(A^T - \hat{A}^T) K_p \tilde{\varsigma} = Y(\varsigma(t), q(t))\tilde{\theta}, \tag{34}$$

where $\tilde{\theta} = \hat{\theta} - \theta$, the dynamics of $\dot{\hat{\theta}}$ is given by

$$\left(\hat{A}^T - A^T\right) K_p \tilde{\varsigma} = Y(\tilde{\varsigma}(t), q(t))\tilde{\theta}, \tag{35}$$

where K_v, K_p are positive-definite velocity and position gain matrices, $\hat{\dot{q}}$ is the estimated velocities of the manipulators by the I&I observer, L and x have been defined in the section of observer design, A is the so-called depth-independent matrix, $Y(\varsigma(t), q(t))$ is a 2×11 matrix, which is only dependent on $\varsigma(t)$ and $q(t)$, θ is an 11-dimension vector about camera parameters.

To prove the stability of the whole system, we firstly substitute the controller into robot system (6), then we have

$$\dot{\hat{\theta}} = \Gamma Y^T(\varsigma(t), q(t)) L(y) x. \tag{36}$$

From the observer design, one has $\hat{x} - x = r\eta + e_x$, so (36) can be transformed into

$$\begin{cases} \dot{y} = Lx \\ \dot{x} = S(y,x)x + L^T\left(-K_v L x - \hat{A}^T K_p \tilde{\varsigma}\right). \\ -L^T K_v L (r\eta + e_x) \end{cases} \tag{37}$$

To analyse the stability of the whole closed-loop system with the control scheme, we define the following Lyapunov-like function,

$$V_4\left(x, \tilde{\varsigma}, \tilde{g}, e_x, e_y, \eta, r\right) = \frac{1}{2}x^T x + \frac{1}{2}C_z \tilde{\varsigma}^T K_p \tilde{\varsigma} + V_2 + \frac{1}{2}r^2 + \frac{1}{2}\tilde{\theta}^T \Gamma^{-1} \tilde{\theta}, \tag{38}$$

https://doi.org/10.1017/S0263574714001015 Published online by Cambridge University Press

where $C_z > 0$. Its time derivative along (14), (25) and (38) is as follows:

$$\begin{aligned}\dot{V}_4 &= x^T\dot{x} + C_z\tilde{\xi}^T K_p\dot{\tilde{\xi}} + \dot{V}_2 + r\dot{r} + \tilde{\theta}\Gamma^{-1}\dot{\tilde{\theta}} \\ &= x^T S(y,x)\,x - x^T L^T K_v L x - x^T L^T \hat{A}^T K_p\tilde{\xi} + \tilde{\theta}\Gamma^{-1}\dot{\tilde{\theta}} \\ &\quad + C_z\tilde{\xi}^T K_p\frac{1}{C_z}A^T L x - x^T L^T K_v L(r\eta + e_x) + \dot{V}_2 + r\dot{r} \\ &= -x^T L^T K_v L x - x^T L^T\left(\hat{A}^T - A^T\right)K_p\tilde{\xi} \\ &\quad - x^T L^T K_v L(r\eta + e_x) + \dot{V}_2 + r\dot{r} + \tilde{\theta}\Gamma^{-1}\dot{\tilde{\theta}}.\end{aligned} \tag{39}$$

With Eqs. (34) and (35), we have

$$\begin{aligned}&\tilde{\theta}^T\Gamma\dot{\tilde{\theta}} - x^T L^T(y)\left(\hat{A}^T - A^T\right)K_p\tilde{\xi} \\ &\quad = \tilde{\theta}^T Y^T(\varsigma(t), q(t))L(y)x - x^T L^T(y)Y(\varsigma(t), q(t))\tilde{\theta} \\ &\quad = 0.\end{aligned} \tag{40}$$

Substituting (40) into (39), one has

$$\begin{aligned}\dot{V}_4 &= -x^T L^T K_v L x - x^T L^T K_v L(r\eta + e_x) + \dot{V}_2 + r\dot{r} \\ &\quad - \lambda_{\min}(K_v)\,|Lx|^2 + \frac{\varepsilon}{2}\,|K_v L x|^2 \\ &\quad + \frac{1}{2\varepsilon}\,|L(r\eta + e_x)|^2 + \dot{V}_2 + r\dot{r} \\ &\quad + \frac{1}{\varepsilon}\,\|L\|^2\,|e_x|^2 - \psi_3\,|\eta|^2 - \psi_4\left|e_y\right|^2 - \psi_5\,|e_x|^2 \\ &\quad + \frac{r^2}{4(1+\psi_3)}\left(\|\triangle_x L\|^2 + \left\|\triangle_y L\right\|^2\right) \\ &= -\left(\lambda_{\min}(K_v) - \frac{\varepsilon}{2}\lambda^2_{\max}(K_v)\right)|Lx|^2 - \psi_4|e_y|^2 \\ &\quad - \left(\psi_3 - \frac{1}{\varepsilon}r^2\,\|L\|^2\right)|\eta|^2 - \left(\psi_5 - \frac{1}{\varepsilon}\,\|L\|^2\right)|e_x|^2 \\ &\quad + \frac{r^2}{4(1+\psi_3)}\left(\|\triangle_x L\|^2 + \left\|\triangle_y L\right\|^2\right).\end{aligned} \tag{41}$$

Note that in the process of derivation of $\dot{V}_4$, we use the Young's inequality $-2ab \le \epsilon a^2 + \frac{1}{\epsilon}b^2$ to get $-x^T L^T K_v L(r\eta + e_x) \le \frac{\varepsilon}{2}\,|K_v L x|^2 + \frac{1}{2\varepsilon}\,|L(r\eta + e_x)|^2$. With (21), there exist $\bar{\triangle}_y$, $\bar{\triangle}_x : R^n \times R^n \times R^n \to R^{n\times n\times n}$ satisfying

$$\begin{aligned}\left\|\triangle_y\left(y, \hat{x}, e_y\right)\right\| &\le \left\|\bar{\triangle}_y\left(y, \hat{x}, e_y\right)\right\|\left|e_y\right| \\ \left\|\triangle_x\left(y, \hat{x}, e_y\right)\right\| &\le \left\|\bar{\triangle}_x\left(y, \hat{x}, e_y\right)\right\|\left|e_x\right|\end{aligned} \tag{42}$$

https://doi.org/10.1017/S0263574714001015 Published online by Cambridge University Press

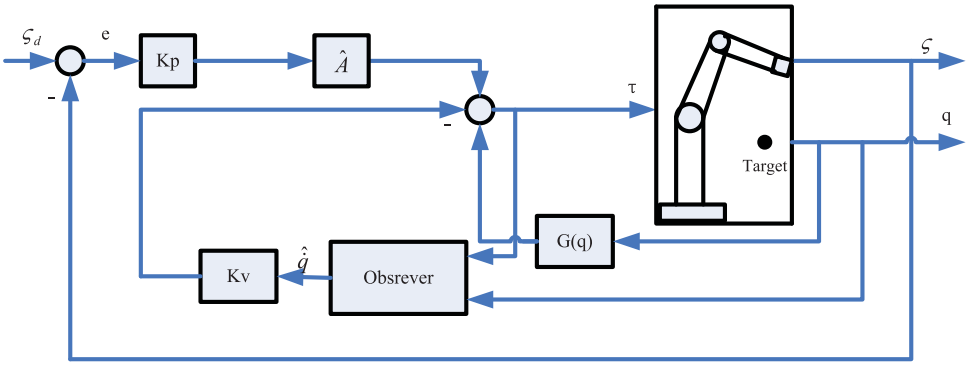

Fig. 1. The block diagram of a closed-loop system.

Then $\dot{V}_4$ yields

$$\begin{aligned}\dot{V}_4 \leq & -\left(\lambda_{\min}(K_v) - \frac{\varepsilon}{2}\lambda_{\max}^2(K_v)\right)|Lx|^2 \\ & -\left(\psi_3 - \frac{1}{\varepsilon}r^2\|L\|^2\right)|\eta|^2 \\ & -\left(\psi_4 - \frac{r^2}{4(1+\psi_3)}\|L\|^2\left\|\bar{\Delta}_y\right\|^2\right)\left|e_y\right|^2 \\ & -\left(\psi_5 - \frac{1}{\varepsilon}\|L\|^2 - \frac{r^2}{4(1+\psi_3)}\|L\|^2\left\|\bar{\Delta}_x\right\|^2\right)|e_x|^2 .\end{aligned} \tag{43}$$

Select the observer parameters as

$$\psi_3 = \frac{1}{\varepsilon}r^2\|L\|^2 + \alpha_1,$$

$$\psi_4 = \frac{r^2}{4(1+\psi_3)}\|L\|^2\left\|\bar{\Delta}_y\right\|^2 + \alpha_2,$$

$$\psi_5 = \frac{1}{\varepsilon}\|L\|^2 + \frac{r^2}{4(1+\psi_3)}\|L\|^2\left\|\bar{\Delta}_x\right\|^2 + \alpha_3,$$

with α_1, α_2, $\alpha_3 > 0$, and ε is chosen such that $0 < \varepsilon < \frac{2\lambda_{\min}(K_v)}{\lambda_{\max}(K_v)}$. Defining $\alpha_0 = \lambda_{\min}(K_v) - \frac{\varepsilon}{2}\lambda_{\max}^2(K_v)$, we have

$$\dot{V}_4 \leq -\alpha_0|Lx|^2 - \alpha_1|\eta|^2 - \alpha_2\left|e_y\right|^2 - \alpha_3|e_x|^2 . \tag{44}$$

With (44), one has $x, \eta, e_y, e_x \in L_\infty \cap L_2$, $r(t) \in L_\infty$, then the closed-loop system is GES. Figure 1 gives the flow chart of the closed-loop system with our control scheme.

With the above analysis, we present the main result as follows.

Theorem 1. Given the robot dynamics (1) and the imaging model (12), the whole system is globally stable with the controller (32), in which the joint velocities are estimated by the observer whose dynamics is obtained from (16), (25) and (27).

Remark 2. To control the 3D position and orientation of a robot manipulator using the visual feedback, more than one feature point must be used in visual servoing. According to the projection geometry of a camera, three non-collinear feature points are sufficient to constrain the position and

https://doi.org/10.1017/S0263574714001015 Published online by Cambridge University Press

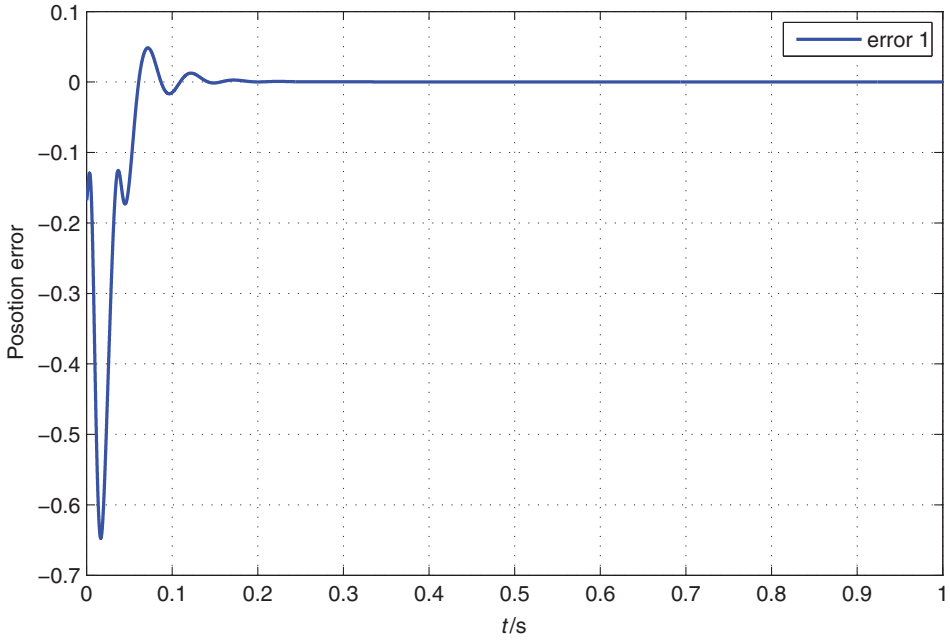

Fig. 2. Position error of joint1 in robot coordinate.

orientation of a rigid object in a 3D space.[13] Similar to Wang *et al.*,[13] the controller proposed in this paper can be directly extended to the tracking control of three feature points. The dimension of the depth-independent interaction matrix will increase the computation time. When three feature points are used, the controller will be designed as follows:

$$\tau = G(q) - K_v \hat{\dot{q}} - \sum_{i=1}^{3} \hat{A}_i^T K_{pi} \tilde{\varsigma}_i \tag{45}$$

Similar to the above proof procedure, by applying the Lyapunov function, the convergence of the image on all the feature points can be proved. The difference is that the convergence of image errors to zero is guaranteed only when three feature points are on the rigid body.

5. Simulations

To illustrate the effectiveness of the proposed control scheme, the simulation results achieved from a two-link camera-to-hand robot will be given in this section. For system (1), the inertial matrix, centripetal and Coriolis matrix and gravitational torque vector are defined as

$$M(q) = \begin{bmatrix} m_1 d_1^2 + m_2 l_1^2 + I_1 & m_2 l_1 d_2 \cos(q_2 - q_1) \\ m_2 l_1 d_2 \cos(q_2 - q_1) & m_2 d_2^2 + I_2 \end{bmatrix},$$

$$C(q, \dot{q}) = \begin{bmatrix} 0 & m_2 l_1 d_2 \sin(q_2 - q_1)\dot{q}_1 \\ m_2 l_1 d_2 \sin(q_2 - q_1)\dot{q}_2 & 0 \end{bmatrix},$$

$$G(q) = \begin{bmatrix} m_1 d_1^2 g \cos(q_1) + m_2 l_1 g \cos(q_1) \\ m_2 d_2 g \cos(q_2) \end{bmatrix},$$

where $m_1 = 2$ and $m_2 = 1.4$ denote the mass of the links, $l_1 = 0.6$ and $l_2 = 0.4$ denote the length of the links, and $d_1 = 0.45$ and $d_2 = 0.3143$ denote the location of the centre of mass of each link from its end. I_1 and I_2 stand for the moment of inertia of the links, these are given by $I_1 = \frac{1}{12} m_1 \left(l_1^2 + l_{wd1}^2\right)$,

https://doi.org/10.1017/S0263574714001015 Published online by Cambridge University Press

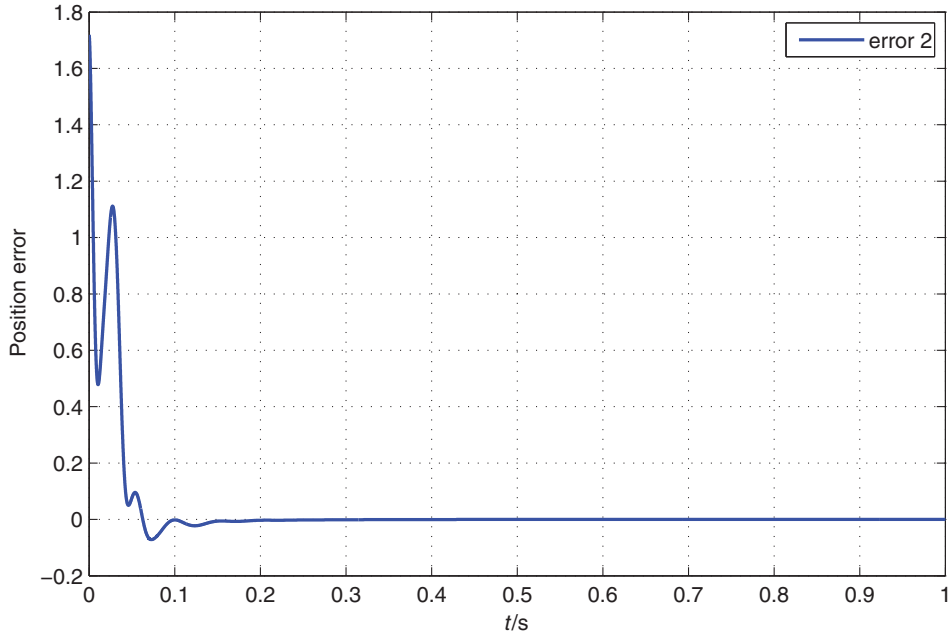

Fig. 3. Position error of joint 2 in robot coordinate.

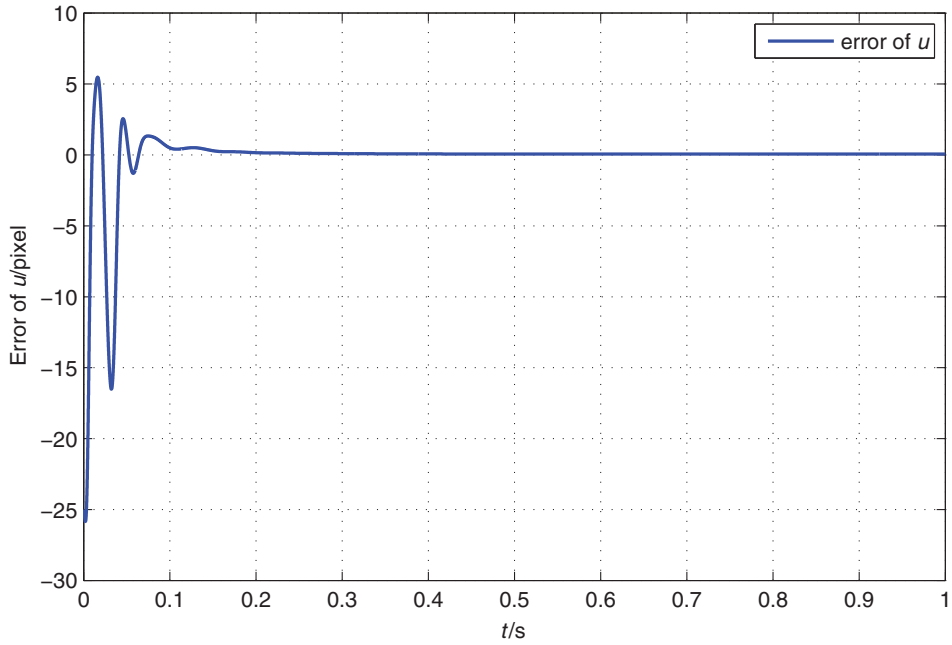

Fig. 4. Position error of u in camera coordinate.

$I_2 = \frac{1}{12} m_2 (l_2^2 + l_{wd2}^2)$, where $l_{wd1} = l_{wd2} = 0.07$ are the width of the links respectively. See ref. [16] for more about the observer dynamics.

The initial estimations of the camera parameters are given as follows,

$$\hat{N}(0) = \begin{bmatrix} 0.97 & -0.26 & 0 & 0.1 \\ 0 & 0 & -1 & 0.1 \\ 0.26 & 0.97 & 0 & 3 \end{bmatrix}.$$

https://doi.org/10.1017/S0263574714001015 Published online by Cambridge University Press

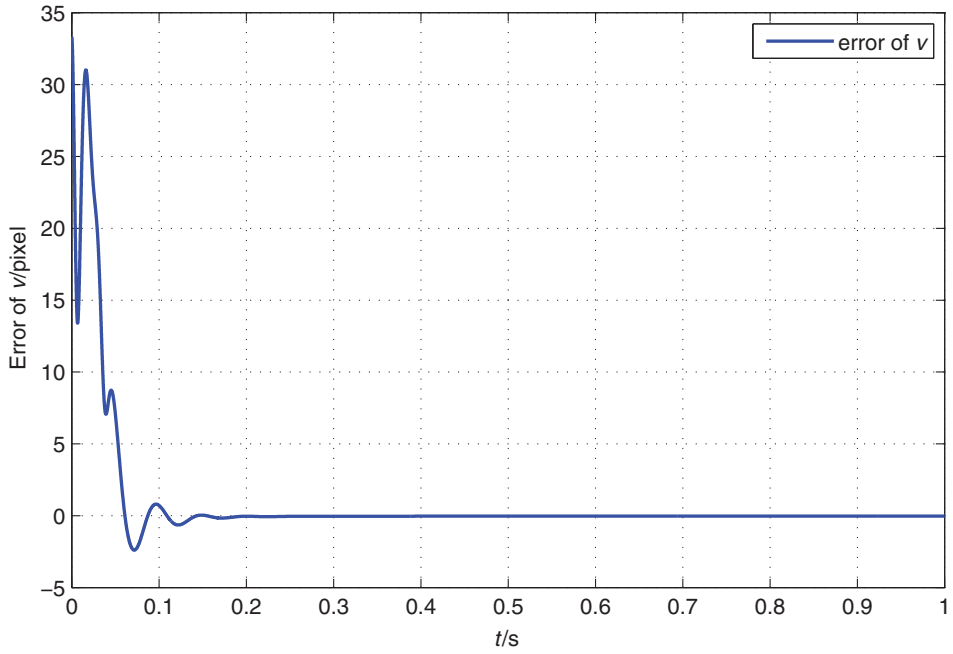

Fig. 5. Position error of v in camera coordinate.

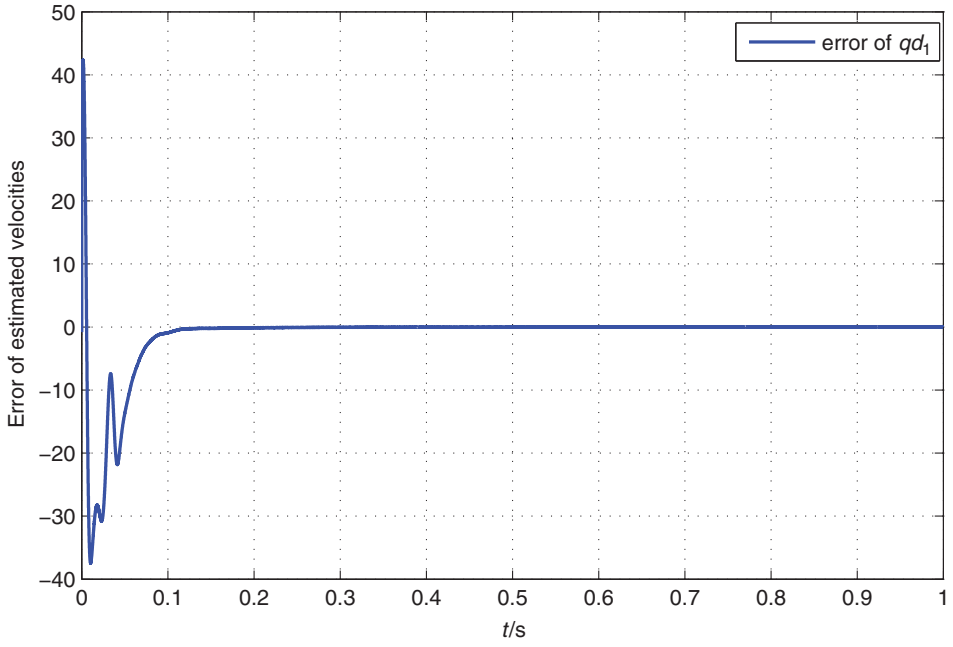

Fig. 6. Estimated error of velocity of joint 1.

Here we select $f = 2, \gamma = 200, p_z = -4$. The initial values of the system are set as $q\,(0) = (0, 0)^T$, $\dot{q}\,(0) = (0, 0)^T$, $\zeta(0) = (30, -40)^T$, $x\,(0) = (3, 4)^T$, $y\,(0) = (1, 2)^T$, $\beta\,(0) = (9.0697, 21.1207)^T$, $r\,(0) = 2$. The controller gains are chosen as $K_p = \text{diag}(5, 8)$, $K_v = \text{diag}(30, 30)$.

The position errors of joints 1 and 2 are shown in Figs. 2 and 3 respectively. Figures 4 and 5 show the position errors with camera coordinates respectively. The estimated errors of joint velocities with our observer are shown in Figs. 6 and 7. From these figures, we can see that all of them converge to zero asymptotically. Therefore, the control objective is achieved by applying the velocity observer and the new controller designed in this paper.

https://doi.org/10.1017/S0263574714001015 Published online by Cambridge University Press

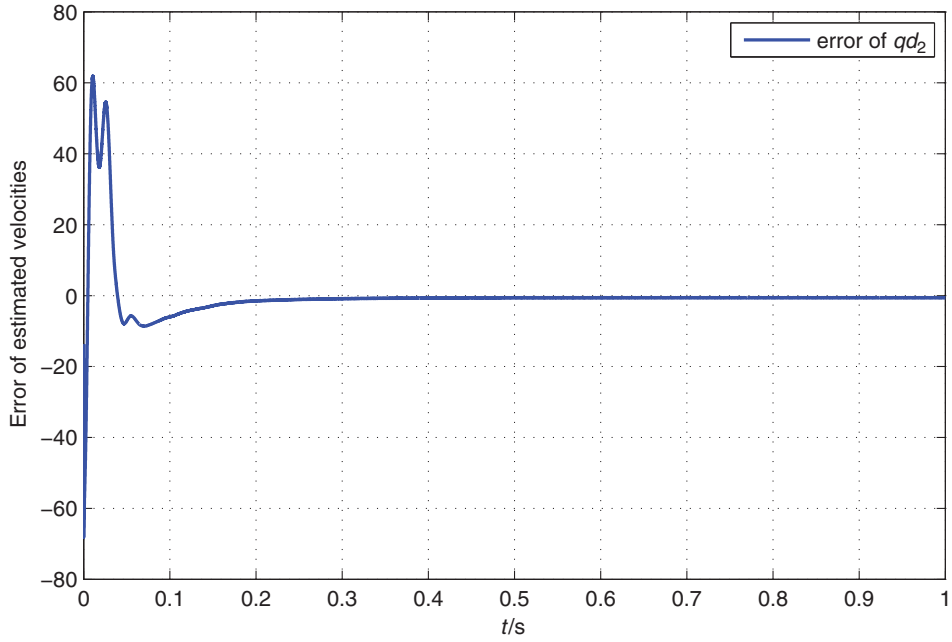

Fig. 7. Estimated error of velocity of joint 2.

6. Conclusions

The image-based robotic control problem is considered with unknown camera parameters and joint velocities in this paper. New observer is designed for the estimation of the unknown velocity information. We use the depth-independent matrix to linearize camera parameters from the image Jacobian matrix and then estimate the unknown camera parameters with adaptive scheme. The observer-based output feedback controller is proposed and the stability of the whole system is proved. Finally, the simulations are performed and the results show the effectiveness of the proposed control methods.

Acknowledgements

This paper is partially supported by the Science Fund for Distinguished Young Scholars of Hebei Province (F2011203110), Hundred Excellent Innovation Talents Support Program of Hebei Province, Doctoral Fund of Ministry of Education of China (20121333110008), Hebei Province Applied Basis Research Project (13961806D) and the National Natural Science Foundation of China (60934003, 61290322, 61273222, 61322303).

References

1. S. Hutchinson, G. Hager and P. Cork, "A tutorial on visual servo control," *IEEE Trans. Robot. Autom.* **12**(5), 651–670 (1996).
2. E. Malis, F. Chaumette and S. Boudet, "Positioning a Coarse-Calibrated Camera with Respect to an Unknown Object by 2D 1/2 Visual Servoing," *Proceedings of the IEEE International Conference on Robotica and Automation*, Leuven, Belgium (1998) pp. 1352–1359.
3. F. Chaumette, "Potential Problems of Stability and Convergence in Image-Based and Position-Based Visual Servoing," *Proceedings of the Confluence of Vision and Control*, Lecture Notes in Control and Information Sciences Volume 237, vol. 237 (1998) pp. 66–78.
4. P. I. Corke and S. A. Hutchinson, "A new partitioned approach to image-based visual servo control," *IEEE Trans. Robot. Autom.* **179**(4), 507–515 (2001).
5. R. Kelly, R. Carelli, O. Nasisi, B. Kuchen and F. Reyes. "Stable visual servoing of camera-in-hand robotic systems," *IEEE Trans. Mechatronics* **5**(1), 39–48 (2000).
6. K. Hashimoto, T. Kimoto, T. Ebine and H. Kimura, "Manipulator Control with Image-Based Visual Servoing," *Proceedings of the IEEE International Conference on Robotics and Automation,* Sacramento, CA (1991) pp. 2267–2272.

https://doi.org/10.1017/S0263574714001015 Published online by Cambridge University Press

7. A. Astolfi, L. Hsu, M. Netto and R. Ortega, "Two solutions to the adaptive visual servoing problem," *IEEE Trans. Robot. Autom.* **18**(3), 387–392 (2002).
8. X. Liang, X. Huang, M. Wang and X. Zeng, "Improved stability results for visual tracking of robotic manipulators based on the depth-independent interaction matrix," *IEEE Trans. Robot.* **27**(2), 371–379 (2011).
9. A. Astolfi and R. Ortega, "Immersion and invariance: A new tool for stabilization and adaptive control of nonlinear systems," *IEEE Trans. Autom. Control* **48**(4), 590–606 (2003).
10. R. A. Maruthi, "Vision-based adaptive tracking control of uncertain robot manipulators," *IEEE Trans. Robot.* **21**(4), 748–753 (2005).
11. Y. H. Liu, H. Wang, C. Wang and K. K. Lam, "Uncelebrated visual servoing of robots using a depth-independent interaction matrix," *IEEE Trans. Robot.* **22**(4), 804–817 (2006).
12. Y. Liu and H. Wang, "Uncelebrated visual tracking control without visual velocity," *IEEE Trans. Control Syst. Technol.* **18**(6), 1359–1370 (2010).
13. H. S. Wang, M. K. Jiang, W. D. Chen and Y. H. Liu, "Visual servoing of robots with uncalibrated robot and camera parameters," *Mechatronics* **22**(6), 661–668 (2012).
14. Y. Su and C. Zheng, "Vision-Based PID Regulation of Robotic Manipulators Without Velocity Measurements," *Proceedings of the IEEE International Conference on Robotics and Automatics*, Tianjin, China (2010) pp. 1698–1703.
15. X. Liang, X. Huang and M. Wang, "Approximate Jacobian Control of Robot Manipulators Without Joint Velocity Measurements," *Proceedings of the IEEE International Conference on Cyber Technology in Automation, Control, and Intelligent Systems*, Kunming, China (2011) pp. 7–12.
16. F. Lizarralde, A. C. Leite, L. Hsu and R. R. Costa, "Adaptive visual servoing scheme free of image velocity measurement for uncertain robot manipulators," *Automatica* **49**(5), 1304–1309 (2013).
17. A. P. Dani, N. R. Fischer, Z. Kan and W. E. Dixon, "Globally exponentially stable observer for vision-based range estimation," *Mechatronics* **22**(4), 381–389 (2012).
18. C. Hua, Y. Liu and J. Leng, "Visual-Based Robotic Control Without Joint Velocities," *Proceedings of the 12th International Conference on Control, Automation, Robotics & Vision* (2012) pp. 1262–1267.
19. A. Astolfi, R. Ortega and A. Venkatraman. "A Globally Exponentially Convergent Immersion and Invariance Speed Observer for N Degrees of Freedom Mechanical Systems," *Proceedings of the IEEE Conference on Decision and Control* (2009) pp. 6508–6513.